TECHNICAL PAPER

ISSN:1047-3289 *J. Air & Waste Manage. Assoc.* **59**:37–44
DOI:10.3155/1047-3289.59.1.37

Modeling Regional/Urban Ozone and Particulate Matter in Beijing, China

Joshua S. Fu
Department of Civil and Environmental Engineering, University of Tennessee, Knoxville, TN

David G. Streets
Decision and Information Sciences Division, Argonne National Laboratory, Argonne, IL

Carey J. Jang
Office of Air Quality Planning and Standards, U.S. Environmental Protection Agency, Research Triangle Park, NC

Jiming Hao, Kebin He, and Litao Wang
Department of Environmental Science and Engineering, Tsinghua University, Beijing, China

Qiang Zhang
Decision and Information Sciences Division, Argonne National Laboratory, Argonne, IL

ABSTRACT

This paper examines Beijing air quality in the winter and summer of 2001 using an integrated air quality modeling system (Fifth Generation Mesoscale Meteorological Model [MM5]/Community Multiscale Air Quality [CMAQ]) in nested mode. The National Aeronautics and Space Administration (NASA) Transport and Chemical Evolution over the Pacific (TRACE-P) emission inventory is used in the 36- (East Asia), 12- (East China), and 4-km (greater Beijing area) domains. Furthermore, we develop a local Beijing emission inventory that is used in the 4-km domain. We also construct a corroborated mapping of chemical species between the TRACE-P inventory and the Carbon Bond IV (CB-IV) chemical mechanism before the integrated modeling system is applied to study ozone (O_3) and particulate matter (PM) in Beijing. Meteorological data for the integrated modeling runs are extracted from MM5. Model results show O_3 hourly concentrations in the range of 80–159 parts per billion (ppb) during summer in the urban areas and up to 189 ppb downwind of the city. High fine PM ($PM_{2.5}$) concentrations (monthly average of 75 $\mu g \cdot m^{-3}$ in summer and 150 $\mu g \cdot m^{-3}$ in winter) are simulated over the metropolitan and downwind areas with significant secondary constituents. A comparison against available O_3 and PM measurement data in Beijing is described. We recommend refinements to the developed local Beijing emission inventory to improve the simulation of Beijing's air quality. The 4-km modeling configuration is also recommended for the development of air pollution control strategies.

IMPLICATIONS

This study develops a new modeling procedure for application to Beijing, China. Refinements to the local Beijing emission inventory beyond TRACE-P inventory are needed to improve the simulation of Beijing's air quality. Obtaining reliable $PM_{2.5}$ monitoring data is essential. Our model can be particularly useful in air quality management plans. The 4-km modeling configuration is also recommended for the development of cost-effective air pollution control strategies.

INTRODUCTION

Beijing, the capital of China, is challenged by rapid economic growth and high demands for energy resulting in large part from the exponentially increasing number of cars. The air quality is of critical concern because concentrations of pollutants such as ozone (O_3) and particulate matter (PM) remain high in Beijing. Government efforts to control air pollution were initiated in the latter part of 1990, yet the improvements have been made only gradually. According to the Beijing Environmental Protection Bureau (BJEPB) report,[1] O_3 concentrations exceeded the China National Ambient Air Quality Standard (CNAAQS; current national standards are Grade II : O_3 = 100 parts per billion [ppb], coarse PM [PM_{10}] = 150 $\mu g \cdot m^{-3}$) for 101 days in 1998. The urban residential areas showed observed 100-ppb hourly O_3 (Grade II standard) during this time period in summer with a maximum hourly observed concentration of 192 ppb. In 2005, data from BJEPB revealed that O_3 concentrations exceeded the Grade II standard for 57 days with a maximum hourly value up to 212 ppb. In recent years, many measurements of PM in Beijing found average summer daily PM_{10} concentrations ranging from 94 to 251 $\mu g \cdot m^{-3}$, often exceeding China's Grade II standard (150 $\mu g \cdot m^{-3}$). Occasionally, daily PM_{10} concentrations have exceeded China's Grade III standard of 250 $\mu g \cdot m^{-3}$. Average daily

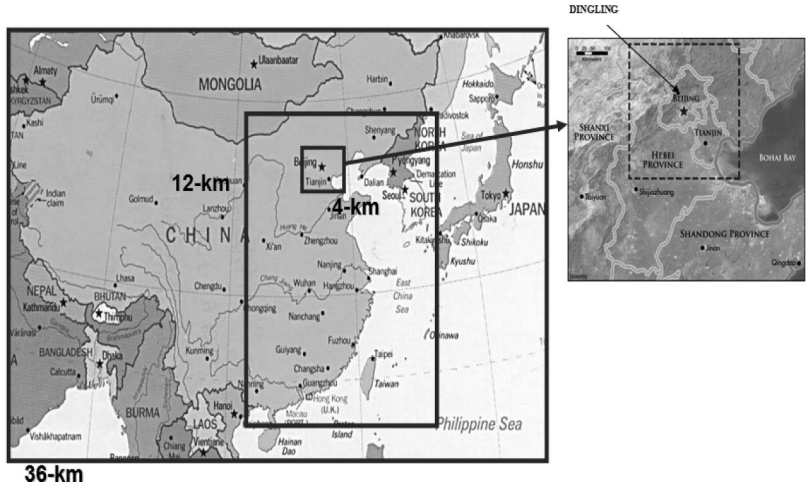

Figure 1. Greater China and Beijing 4-km modeling domains.

fine PM ($PM_{2.5}$) concentrations measured in recent studies[2] ranged from 75 to 169 $\mu g \cdot m^{-3}$ and were well above the U.S. National Ambient Air Quality Standards value of 65 $\mu g \cdot m^{-3}$. Numerous groups have conducted PM measurements; however, few O_3 measurement studies have been reported for the greater Beijing area.[2] Furthermore, modeling studies of O_3 and $PM_{2.5}$ in Beijing are scarce; to date, environmental modeling has only been conducted by Wang and Li in 2000 (reported in Chinese journals)[3,4] and summarizing reports.[5]

Se have undertaken a study to conduct a regional modeling assessment by developing a premier integrated modeling system that links a regional chemical transport model (Models-3/Community Multiscale Air Quality [CMAQ]),[6,7] and a meteorological model (Fifth Generation Mesoscale Meteorological Model [MM5]),[8] and applying it to the Greater China region. This is the first attempt to model O_3 and PM with such an integrated modeling system over China. This study focuses on the greater Beijing area, including neighboring cities such as Tianjin and the adjacent provinces Hebei, Shandong, and Shanxi (Figure 1). To facilitate the use of the modeling system for this study, it is essential to obtain high-quality emission inventories for China. The O_3 and PM data must accurately reflect variability in emissions in the study area to be modeled.

The focus of this paper is twofold: (1) to apply the Models-3/CMAQ and MM5 models in an integrated framework to establish the feasibility of simulating O_3 and PM in Beijing, and (2) to identify the causes for high O_3 concentrations in July 2001 and high PM concentrations in January and July 2001. The present literature is limited in demonstrating the application of modeling in the Beijing area, particularly O_3 modeling. This study shows promise for providing China's research groups with a sophisticated modeling capability to investigate the characteristics of air quality in China.

METHODS

We currently use an advanced modeling system with a "one-atmosphere" perspective, the U.S. Environmental Protection Agency's Models-3/CMAQ modeling system.[6,7] The numerical modeling system of Models-3/CMAQ simultaneously simulates the transport, physical transformation, and chemical reactions of multiple pollutants across large geographic regions. The system is useful to states and other government and international agencies for making regulatory decisions on air quality management, as well as to research scientists for performing atmospheric research. As a result, this integrated approach allows us to model multiple air quality issues at various scales for such issues as O_3, PM, visibility degradation, acid deposition, and air toxics. Furthermore, the modular design of CMAQ allows the user to build different chemistry transport models for simulating various air quality scenarios.

Model Domain

On the basis of the Lambert Conformal map projection centered at (34 °N, 110 °E), the model domain covers the Greater China region including Beijing. Figure 1 shows the nested grids at 36- by 36-km (D1), 12- by 12-km (D2), and 4- by 4-km (D4) resolutions set up by the MM5 meteorological processing model. There are 164 × 97 horizontal grid cells in D1, 175 × 211 in D2, and 90 × 90 in D4. Fourteen vertical layers are configured following the Sigma (σ) layer structure with more vertical layers near the surface to better resolve the boundary layers. The 14-layer interfaces occur at: 1 (0 m), 0.995 (38 m), 0.988 (92 m), 0.98 (153 m), 0.97 (230 m), 0.956 (340 m), 0.938 (482 m), 0.893 (846 m), 0.839 (1300 m), 0.777 (1850 m), 0.702 (2557 m), 0.582 (3806 m), 0.400 (6083 m), 0.20 (9511 m), and 0.00 (16,262 m).

Meteorology

MM5 v3.7[8] is used to provide meteorological input fields for the model simulations. The 36-, 12-, and 4-km domains and their meteorological outputs simulated by MM5 in the Greater Asia modeling effort[9] were used in this work. The Meteorology/Chemistry Interface Processor (MCIP) 2.2 model[6] is used to process the MM5 output data into the format and structure required by the CMAQ model. Basic structures, schemes, and relevant parameters of the CMAQ and MM5 models are shown in Table 1.

Table 1. Basic structures, schemes, and relevant parameters of the CMAQ and MM5 models

Models	CMAQ
Horizontal resolution	36, 12, and 4 km
Vertical resolution	14 σ_p levels
Depth of first layer	38 m
Model top	16 km
Projection	Lambert
Meteorology	MM5/NCAR-PSU
	Terrain: USGS data
	Observation: NCEP
	Physics: Kain-Fritsch cumulus schemes[24]
	PBL: Blackadar scheme[25]
	Mix phase explicit moisture schemes[26]
	Cloud atmospheric radiation scheme[27]
	Force/restore surface scheme: Blackadar[28,29]
Advection	Piecewise parabolic
Vertical diffusion	K-theory
Dry deposition	Wesely [30]
Wet scavenging	Henry's law
Gas chemistry	CB-IV
Aqueous chemistry	Walcek[31]

Notes: PSU, Pennsylvania State University; USGS, U.S. Geological Survey; NCEP, National Centers for Environmental Protection.

Emission Estimates

Inventories of 11 major chemical species, initially gridded at 2′ (4 km), 6′ (12 km), and 18′ (36 km) resolutions, have been developed by the Transport and Chemical Evolution over the Pacific (TRACE-P) project. This inventory includes sulfur dioxide (SO_2), oxides of nitrogen (NO_x), carbon dioxide (CO_2), carbon monoxide (CO), methane (CH_4), non-methane volatile organic compounds (NMVOCs), black carbon aerosol (BC), organic carbon aerosol (OC), ammonia (NH_3), PM_{10}, and $PM_{2.5}$. The biogenic emission inventory from the Global Emissions Inventory Activity (GEIA; an inventory from the International Geosphere-Biosphere Program [IGBP], www.geiacenter.org/) was also included. Detailed emissions are considered by type of fossil fuel for the sectors of anthropogenic combustion, which are aggregated into five primary source categories of industry, residential, transportation, power generation, and agriculture. Biomass burning is calculated independently in three major categories: forest burning, savanna/grassland burning, and the burning of crop residues. Emission inventories are updated to year 2000 for each country in Asia and for each province of China.[10] However, the total annual emissions of these 11 pollutants and the 18 subcategories of NMVOCs developed by the TRACE-P project are not directly compatible with the Carbon Bond IV (CB-IV) chemical mechanism that utilizes 22 chemical species in CMAQ. Different species of NMVOCs were merged into higher aldehyde bases such as acetaldehyde (ALD2), ethane (ETH), formaldehyde (FORM), olefin carbon bond (OLE), paraffin carbon bond (PAR), toluene and other monoalkyl aromatics (TOL), and xylene and other polyalkyl aromatics (XYL). $PM_{2.5}$ and PM_{10} were divided into fine aerosols on the basis of the speciation profile developed by the U.S. Environmental Protection Agency (EPA) (used by the Sparse Matrix Operator Kernal Emission [SMOKE] model,[11] including the chemical speciation profiles [GSPRO] and speciation cross-reference [GSREF]). Biogenic isoprene (ISOP) and terpenes (TERPB) were directly prepared by geographic information systems (GIS) based on land-use information.[12] Only domestic, agriculture, biomass burning, and biogenic sectors are assumed to have seasonal variations in China in the TRACE-P project. Monthly operation hours of stoves for domestic heating were estimated based on monthly mean temperatures for each province in China. Combustion emissions for the domestic sector in January and July were estimated based on the monthly profiles of stove hours. The TRACE-P project provided the weekly and hourly profiles[9] for emission processes. On the basis of a list of chamber studies and chemical reactions,[13–17] the TRACE-P species were mapped to the CB-IV chemical mechanism in Table 2. To model the 4-km inner domain in the greater Beijing area, the TRACE-P values, which were primarily developed for regional- and continental-scale modeling, were replaced by an updated local inventory for the eight districts in the city of Beijing.

Initial and Boundary Conditions

The nest-down boundary conditions for the 12- and 4-km simulations were provided by the parent 36-km CMAQ domain. The clean-air background assumption is invalid for these modeling applications, so the initial and boundary conditions for the 36-km domain were obtained from global chemical transport model (GEOS-Chem) results.[18]

Air Pollution Index (API) Calculation

PM_{10} and O_3 concentrations are calculated using the API published by the Beijing Municipal Environmental Protection Bureau. The API grading standard for urban air quality is based on a daily average and is shown in Table 3. The API of a certain pollutant is calculated by the equation:

$$I = \frac{I_{\text{high}} - I_{\text{low}}}{C_{\text{high}} - C_{\text{low}}} \quad (C - C_{\text{low}}) + I_{\text{low}} \qquad (1)$$

in which C_{high} and C_{low} are the two grading concentrations (between two pollutant index), such as 0.05 and 0.15 mg/cm^{-3} for SO_2 daily average concentrations in the Table 3, near the observed concentration C. I_{high} and I_{low} are the corresponding pollutant indices of the two grading concentrations, such as 50 and 100 in Table 3. Therefore, we can calculate the concentrations from the published API according to Table 3 and the above equation.

RESULTS AND DISCUSSION

The climate in China is characterized by an Asian continental outflow in winter and a maritime breeze during the summer. The winter climate typically exhibits north to northwesterly winds over the eastern part of China, which includes Beijing. However, the summer climate is characterized by prevalent south to southeasterly winds from the East Sea and the Yellow Sea. Consequently, areas north of Beijing are dominated by a downwind flow where O_3 can accumulate during the summer. To facilitate better air quality predictions, reasonable temporal allocation and higher geographical precision of emission

Table 2. TRACE-P species mapped to CB-IV.

Trace-P				CB-IV[22]		
No	**Pollutant**	**MW**	**Mapping from Trace-P to CB-IV**		**Pollutant**	**MW**
1	Ethane	30.0	2*[9] + 2.5*[16] + 1.5*[31]	ALD2	Acetaldehyde and higher aldehydes	32
2	Propane	44.0	[23]	CO	CO	28
3	Butanes	58.0	[6]	ETH	Ethene	32
4	Pentanes	72.0	[15]	FORM	Formaldehyde	16
5	Other alkanes	86.0	[30]	ISOP	Isoprene	68.12
6	Ethene	28.0	[27]	NH_3	Ammonia	17
7	Propene	40.0	0.9*[21]	NO	NO	30
8	Terminal alkenes	56.2	0.1*[21]	NO_2	Nitrogen dioxide	46
9	Internal alkenes	56.2	1.6*[1] + 1.5*[2] + 1.5*[10] + [24] + 0.5*[32]	NR	Nonreactive carbon	–
10	Acetylene	26.0	[7] + [8] + 0.5*[32] + 0.5*[31]	OLE	Olefinic carbon bond (C=C)	32
11	Benzene	78.0	0.4*[1] + 1.5*[2] + 4*[3] + 5*[4] + 6*[5] + [7] + 2*[8] + 1.5*[10] + 8.5*[32] + [11] + 4*[17] + 1.33*[19] + 6*[31]	PAR	Paraffin carbon bond (C=C)	16
12	Toluene	92.0	[25]	PEC	Primary EC	–
13	Xylenes	106.0	[29] - [28]	PMC	Coarse-mode PM (PM_{10} minus $PM_{2.5}$)	–
14	Other aromatics	117.0	[28] - [25] - [26] -PNO_3 - PSO_4	PMFINE	Fine-mode PM (other)	–
15	Formaldehyde	30.0	[28]*X	PNO_3	Primary nitrate aerosol	–
16	Other aldehydes	88.0	[26]	POA	Primary organic aerosol	–
17	Ketones	126.0	[28]*X	PSO_4	Primary sulfate aerosol	–
18	Halocarbons	150.0	[20]	SO_2	SO_2	64
19	Other	72.0	0.02*[20]	SULF	Sulfuric acid	96
20	SO_2	64.0	[31]	TERPB	Monoterpenes	114
21	NOx	46.0	[12] + 0.5*[14]	TOL	Toluene (C_6H_4-CH_3)	112
22	CO_2	44.0	[13] + 0.5*[14]	XYL	Xylene (C_6H_5-$(CH_3)_2$)	128
23	CO	28.0				–
24	CH_4	16.0				–
25	BC	12.0				–
26	OC	12.0				–
27	NH_3	17.0				–
28	$PM_{2.5}$					–
29	PM_{10}					–
30	ISOP (biogenic, GEIA)	5 carbons				–
31	TERP (biogenic, GEIA)	10 carbons				–
32	Other VOCs (biogenic, GEIA)	10 carbons				–

Notes: X will depend on sectors of SCC—same as CB-IV scheme.

sources are necessary. As Figure 2 indicates, the amount of NO_x emissions is typically (20%) higher in winter than in summer because of increased energy demand during the cold weather conditions. The importance of spatial allocation is also demonstrated in the same figure with paraffin emissions (one of CB-IV's aggregated volatile organic compound [VOC]) species), which are more diffuse with local emissions around Beijing City.

The local emission inventory has higher emissions of NO_x (by 45%) and VOCs (by 24%) within the greater Beijing area than does the TRACE-P inventory. As a result, predicted O_3 concentrations are higher when the local inventory is used (Figure 3), and high O_3 concentrations are more widely distributed north of Beijing. The site of the 2008 Summer Olympic Games is located between the fourth and fifth ring roads, due north of the city center of Beijing, where the peak O_3 occurs at 159 ppb. We also find higher O_3 concentrations at Dingling, an area 50 km north of Beijing and downwind from Beijing. Figure 4 shows that high predicted O_3 concentrations occurred at

Table 3. The API value and corresponding pollutant concentrations.

	Pollutant Concentrations (mg/m^3)				
API	**SO_2 (daily average)**	**NO_2 (daily average)**	**PM_{10} (daily average)**	**CO (hourly average)**	**O_3 (hourly average)**
50	0.050	0.080	0.050	5	0.120
100	0.150	0.120	0.150	10	0.200
200	0.800	0.280	0.350	60	0.400
300	1.600	0.565	0.420	90	0.800
400	2.100	0.750	0.500	120	1.000
500	2.620	0.940	0.600	150	1.200

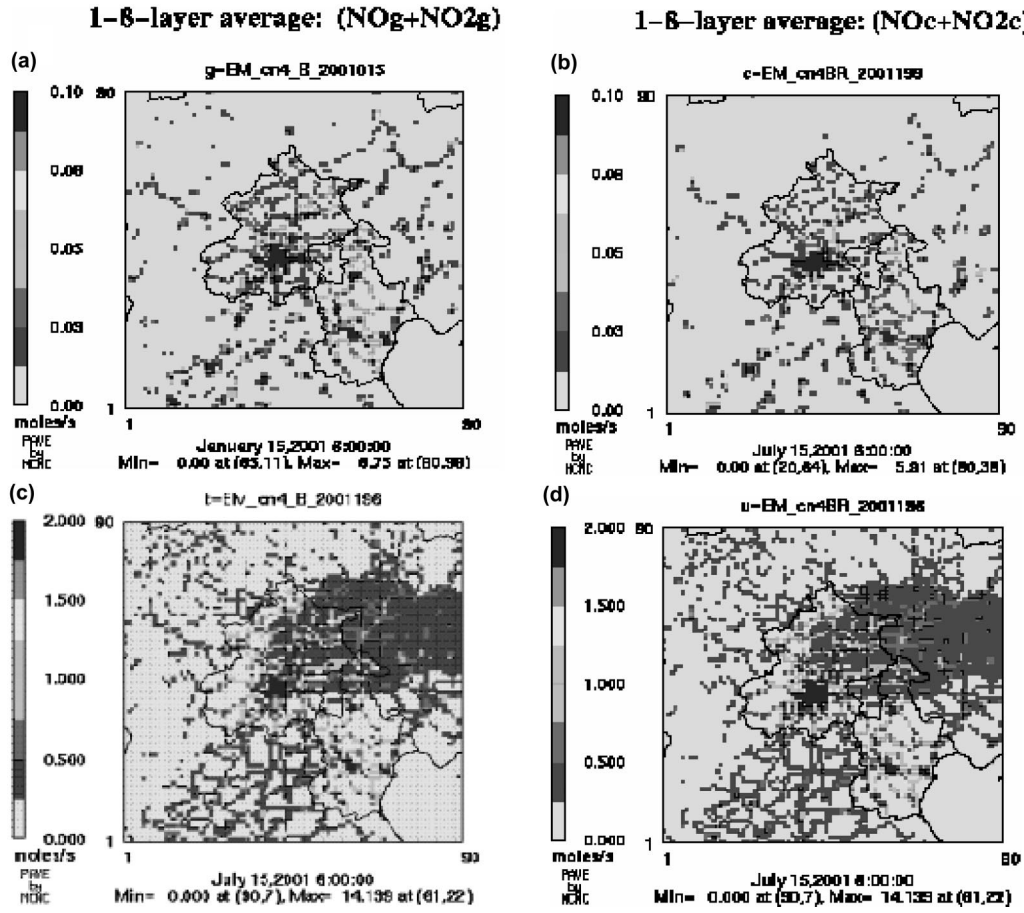

Figure 2. (a) NO_x emissions in January and (b) July 2001. (c) Paraffin emissions (one of CB-IV aggregated VOC species) from TRACE-P. (d) Beijing local emission database. All are on 4-km Beijing domain.

Dingling on July 11 (179 ppb), July 15 (164 ppb), July 20 (159 ppb), and July 23 (137 ppb), 2001. During this period, southerly winds prevailed over the whole domain with noted high wind speed, resulting in O_3 transport to the downwind area. At the Olympic Stadium site in Beijing, the simulated maximum O_3 concentration occurs on July 6 at 119 ppb, whereas a lower O_3 concentration occurred at Dingling on that date, likely because of the northerly wind transporting NO_x and O_3 to the city center of Beijing, as shown in Figure 4. This resulted in an O_3 peak downwind of the urban areas. Wang and Li in the Chinese literature report that monitor data show maximum O_3 concentrations of 195 ppb at Peking University (PKU) and 210 ppb at the Ming Tombs site in late June 2000.[4] Over the same period of time, Wang and Li report that their model simulations yielded an O_3 concentration range of 70–90 ppb within the city at 2:00 p.m. local time on June 26, 2000.[3] Using their simulation-to-observation ratio of 0.813, the average downtown O_3 concentration can be as high as 110 ppb. Zhang et al.[19] report that O_3 concentrations within the city often vary between 50 and 100 ppb, and greater than 100 ppb for areas outside of the city. The maximum predicted O_3 concentration of 159 ppb is underestimated if compared with the published and unpublished literature and data, even when local Beijing emissions are used; however, the spatial distribution of O_3 is consistent with the measurements. A higher O_3 concentration was measured in summer 2005 at a rural, mountainous site north of Beijing,[20] which is consistent with predictions from current CMAQ modeling. It is evident that a south to southeasterly maritime breeze makes the regions north of Beijing a downwind area. With ample sunlight in summer, photochemical reactions take place more efficiently. Because the O_3 precursors NO_x and VOCs are mainly emitted in Beijing and adjacent cities in the south and southeast, O_3 accumulates north of Beijing when there is a southerly wind, which is typical during the summer in Beijing. These transport effects have been reproduced in this research and in Streets et al.[2] The NO_x/VOC ratio in Beijing City is 2 to 3 times higher than most of the major cities on the U.S. East Coast, which could be caused by underestimation of VOC emissions.[3] Thus, the closer estimation of uncertainty in VOC emissions should be taken into account or O_3 predictions may be underestimated because of O_3 titration by nitric oxide (NO) in Beijing. We conclude that the simulated O_3 production in July corresponds well with the observation data[3] depicted in Figures 3 and 4.

Figure 5 depicts the modeled monthly average $PM_{2.5}$ concentration in the greater Beijing area during winter and summer 2001. It is not surprising that the $PM_{2.5}$ concentration in winter is twice that of summer. Measurements of $PM_{2.5}$ indicate similar winter-to-summer ratios.[21,22] High $PM_{2.5}$ concentrations correspond to the higher demand for heat and energy in winter. Simulations for January 2001 gave rise to a monthly average of 150

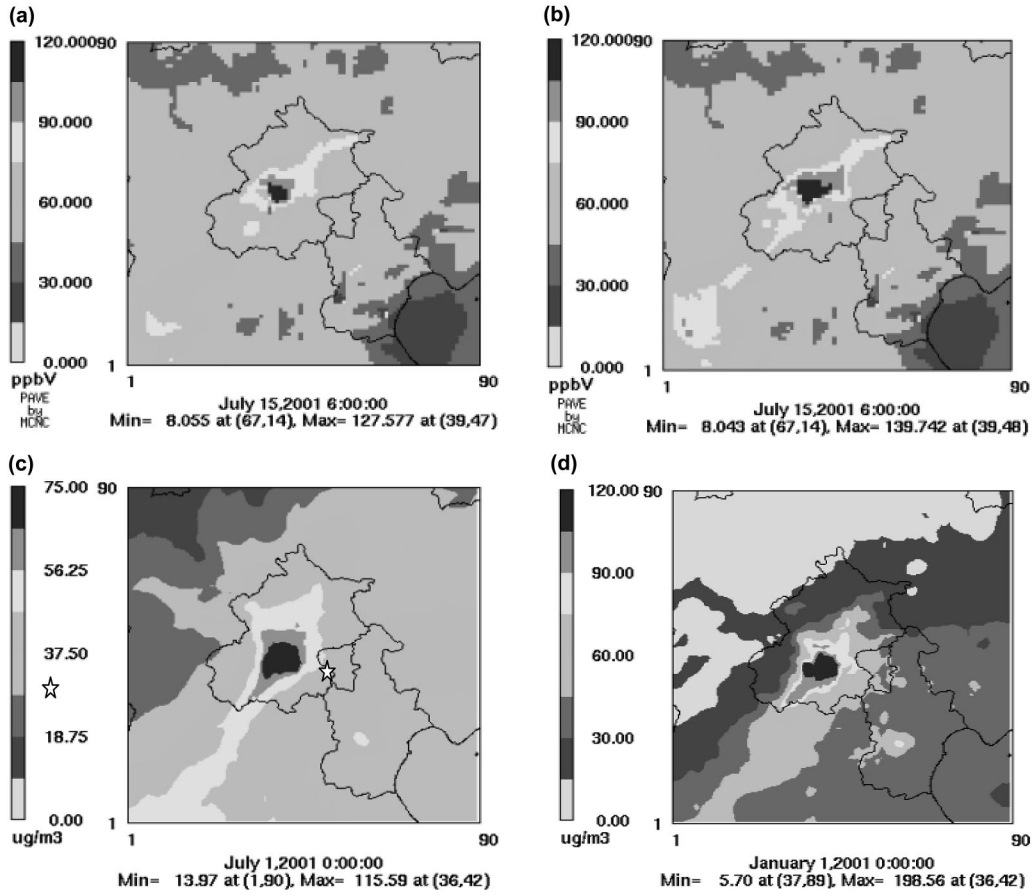

Figure 3. Maximal hourly O_3 concentration using (a) TRACE-P emissions and (b) Beijing local emissions. Monthly average $PM_{2.5}$ episode averages concentrations in (c) January and (d) July 2001. Star represents the city center of Beijing.

$\mu g \cdot m^{-3}$ in the modeled domain in Figure 1. The daily maximum $PM_{2.5}$ concentration of 162 $\mu g \cdot m^{-3}$ occurs on January 18. The simulated $PM_{2.5}$ concentration is considerably lower than that measured by Dan et al.,[20] in which they reported a December 2001 $PM._{2.5}$ average of 257

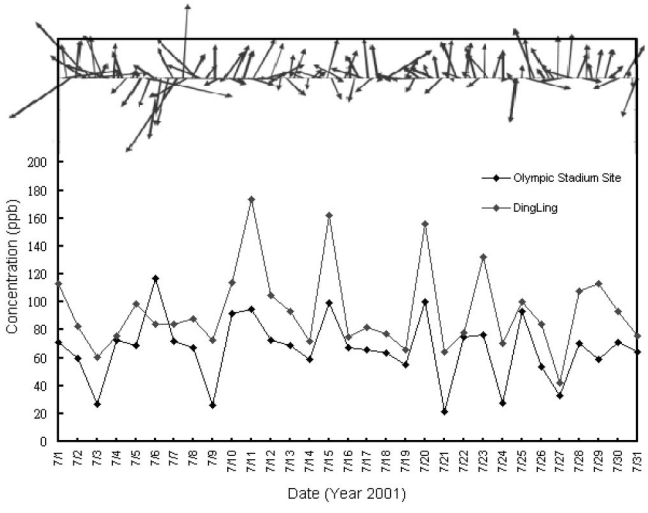

Figure 4. CMAQ model simulations of maximum daily O_3 concentrations at the Olympic Stadium site and Dingling (north of Beijing about 50 km in Figure 1) in Beijing for July 2001. The red vectors represent wind directions and wind speeds.

$\mu g \cdot m^{-3}$ at Beijing Normal University (BNU), located in the western part of downtown Beijing. Figure 3d shows a northeast-southwest elongation of the $PM_{2.5}$ maximum, which extends across the BNU site. The fraction of predicted $PM_{2.5}$ contributed by OC is 18% for January 2001, which is consistent with field data from Dan et al., in which they reported an OC fraction of 16%. Elemental carbon (EC) contributions are also similar between the simulations and the observations (10 and 11%, respectively). The monthly average $PM_{2.5}$concentration was calculated over the city of Beijing for July 2001. Composition of the $PM_{2.5}$ indicates that 17% of the average $PM_{2.5}$ concentration of 75 $\mu g \cdot m^{-3}$ was contributed by OC and 10% by EC. The relative contribution by OC is quite similar when compared with measurements of 19% at BNU. The 10% EC generated by the model is moderately higher than the 4% at BNU.[20] O_3 and $PM_{2.5}$ source apportionment studies in the Beijing metropolitan areas were conducted by Yu et al.[23] during the summer of 2006. Their observations reveal that biomass burning, coal combustion, and industry make up 11, 19, and 6% of the $PM_{2.5}$ composition, respectively. Because these are major sources of OC, the result is consistent with observations and model results from summer 2001. However, the simulated monthly average $PM_{2.5}$ concentration is lower than the concentration of 104 $\mu g \cdot m^{-3}$ measured at BNU,[20] and also lower than the average of 93 $\mu g \cdot m^{-3}$ taken over five urban and rural

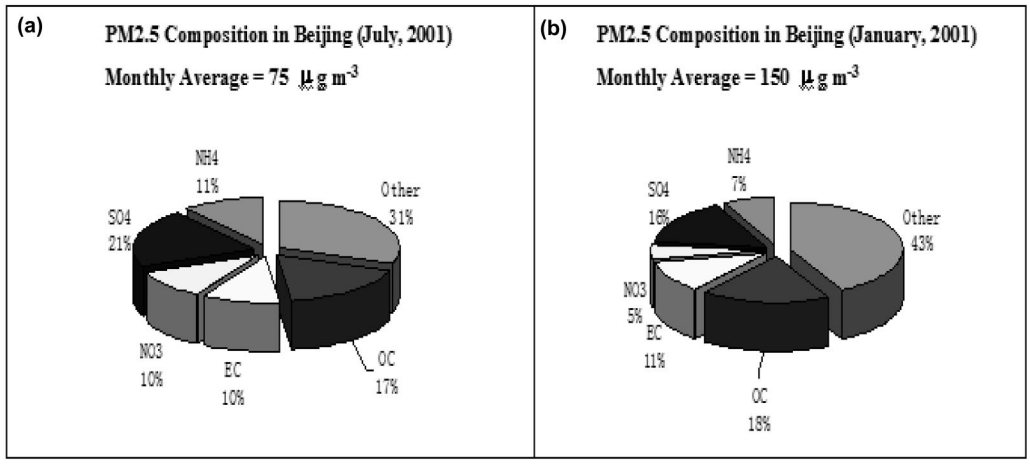

Figure 5. Monthly average modeled $PM_{2.5}$ composition in Beijing in (a) July and (b) January 2001.

sites.[21] This suggests that the model is able to capture the $PM_{2.5}$ composition in the region as well as the spatial patterns of the $PM_{2.5}$ in both seasons. The underestimation in the simulations may be associated with missing emissions such as NO_x and VOC emissions in the TRACE-P and local inventories.

Similarly, the daily maximum PM_{10} concentrations for July 2001 are also compared with API-derived observations. PM_{10} concentrations show a negative bias, consistent with an underestimation of the magnitude of PM_{10}. Uncertainties in VOC emissions and in organic aerosol production may be heavily influencing the PM_{10} predictions in the previous section as Streets et al. discussed.[2] Nevertheless, the model correctly represents processes that contribute to PM_{10} accumulation, because the overall trend is consistent with the API record. Winds from the south also play an important role in the PM_{10} concentrations. Streets et al. demonstrate that weak south winds are favorable for regional transport of particulates from neighboring provinces.[2]

CONCLUSIONS

We have developed the first integrated modeling system on the basis of a MM5/Models-3/CMAQ application by using initial and boundary conditions provided by the GEOS-Chem global chemistry transport model to establish the feasibility of simulating the regional air pollutants of O_3 and $PM_{2.5}$ in the greater Beijing area. We also constructed a corroborated mapping of chemical species in TRACE-P to the CB-IV chemical mechanism. Simulated O_3 concentrations ranged from 80 to 159 ppb in the urban areas during summer. The model results are consistent with measurements that show high O_3 concentrations in summertime in the mountains to the north (Dingling) of Beijing, which is downwind of the urban center amid south to southeasterly maritime breezes. With ample sunlight in summer, O_3 precursors in Beijing and adjacent cities in the south and southeast further enhance O_3 concentrations in the north. The NO_x/VOC ratio in Beijing City is 2–3 times higher than most of the major cities on the U.S. East Coast, which could be because of underestimated VOC emissions. As such, the uncertainty in VOC emissions should be considered for O_3 predictions that may be underestimated because of O_3 titration by NO. We conclude that the simulated O_3 production by using the advanced modeling system in July captures the typical trend and spatial distribution of O_3 in Beijing in the summer months, but tends to underestimate the extreme O_3 concentrations that were observed.

Monthly average $PM_{2.5}$ (75 $\mu g \cdot m^{-3}$ in summer and 150 $\mu g \cdot m^{-3}$ in winter) concentrations are also reported for the metropolitan and downwind areas. The CMAQ model predicts $PM_{2.5}$ concentrations in the winter that are twice as high as concentrations in the summer, which is consistent with observations. The model also captures the observed composition and spatial patterns of $PM_{2.5}$. However, the model underestimates the API-derived $PM_{2.5}$ concentrations. It is possible that the API-derived values are not correct because of the approximations of the published API data from ranges of the leveled concentrations in the API table. Uncertainties in both the TRACE-P and local emissions may be contributing to model underestimates as well. With reliable $PM_{2.5}$ monitoring data, we recommend refinements to the local Beijing emission inventory to improve the simulation of Beijing's air quality. Our model can be particularly useful in developing air quality management plans. The 4-km modeling configuration is also recommended for the development of cost-effective air pollution control strategies with reliable model settings.

ACKNOWLEDGMENTS

This work was funded by EPA's Intercontinental Transport and Climatic Effects of Air Pollutants (ICAP) project and STAR R830959 (GCAP) grants. We thank Rokjin Park for providing GEOS-Chem 2001 data. We also thank anonymous reviewers who spent much time and provided very thoughtful suggestions to make this manuscript more readable.

REFERENCES

1. Hao, J.; Wang, L. Improving Urban Air Quality in China: Beijing Case Study; *J. Air & Waste Manage. Assoc.* **2005**, *55*, 1298-1305.
2. Streets, D.G.; Fu, J.S.; Jang, C.J.; Hao, J.; He, K.; Tang, X.; Zhang, Y.; Wang, Z.; Li, Z.; Zhang, Q.; Wang, L.; Wang, B.; Yu, C. Air Quality during the 2008 Beijing Olympic Games; *Atmos. Environ.* **2007**, *41*, 480-492.
3. Wang, X.; Li, J. The Contribution of Anthropogenic Hydrocarbons to O_3 Formation in Beijing Areas (in Chinese); *China Environ. Sci.* **2002**, *22*, 501-505.

4. Wang, X.; Li, J. A Case Study of Ozone Source Apportionment in Beijing (in Chinese); *Acta Scientiarum Naturalium, Universitatis Pekinensis* **2003**, *39,* 244-253.
5. Tang, X. *Urbanization, Energy, and Air Pollution in China: the Challenges Ahead—Proceedings of a Symposium*, The National Academies: Washington, DC, 2004.
6. Byun, D.W.; Ching, J. K.S. *Science Algorithm of the U.S. Environmental Protection Agency (EPA) Models-3 Community Multiscale Air Quality (CMAQ) Modeling System*; EPA/600/R-99/030; U.S. Environmental Protection Agency; Office of Research and Development: Washington, DC, 1999.
7. Byun, D.; Schere, K.L. Review of the Governing Equations, Computational Algorithms, and Other Components of the Models-3 Community Multiscale Air Quality (CMAQ) Modeling System; *Appl. Mech. Rev.* **2006**, *59,* 51-77.
8. *MM5 Community Model*; National Center for Atmospheric Research and Pennsylvania State University; 2005; available at *http://www.mmm.ucar.edu/mm5/* (accessed 2008).
9. Fu, J.S.; Jang, C.J.; Streets, D.G.; Li, Z.; Kwok, R.; Park, R.; Han, Z. MICS-Asia II: Evaluating Gaseous Pollutants in East Asia Using an Advanced Modeling System: Models-3/CMAQ System; *Atmos. Environ.* **2008**, *42*, 3571-3583.
10. Streets, D.G.; Bond, T.C.; Carmichael, G.R.; Fernandes, S.D.; Fu, Q.; He, D.; Klimont, Z.; Nelson, S.M.; Tsai, N.Y.; Wang, M.Q.; Woo, J.-H.; Yarber, K.F. An Inventory of Gaseous and Primary Aerosol Emissions in Asia in the Year 2000; *J. Geophys. Res.* **2003**, *108*, 8809.
11. *Sparse Matrix Operator Kernel Emission (SMOKE) Modeling System*; University of North Carolina, Carolina Environmental Programs, Research Triangle Park, NC, 2003.
12. *LandScan*; Oak Ridge National Laboratory of U.S. Department of Energy: Oak Ridge, TN, 2001; available at *http://www.ornl.gov/sci/landscan/* (accessed 2006).
13. Middleton, P.; Stockwell, W.R. Aggregation and Analysis of Volatile Organic Compound Emissions for Regional Modeling; *Atmos. Environ.* **1990**, *24,* 1107-1133.
14. Stockwell, W.R.; Kirchner, F.; Kuhn, M. A New Mechanism for Regional Atmospheric Chemistry Modeling; *J. Geophys. Res.* **1997**, *102*, 847-879.
15. Jacobson, M.Z. *Fundamentals of Atmospheric Modeling*; Cambridge University: Cambridge, U.K., 2000; p 656.
16. Sexton, K. University of North Carolina, Chapel Hill, NC. Personal communication, 2002.
17. Jacobson, M. California Air Research Board, Sacramento, CA. Personal communication, 2002.
18. Heald, C.L.; Jacob, D.J.; Fiore, A.M.; Emmons, L.; Gille, J.C.; Sachse, G.W.; Browell, E.V.; Avery, M.A.; Vay, S.A.; Crawford, J.H.; Westberg, D.J.; Blake, D.R.; Singh, H.B.; Sandholm, S.T.; Talbot, R.W.; Fuelberg, H.E. Asian Outflow and Transpacific Transport of Carbon Monoxide and Ozone Pollution: an Integrated Satellite, Aircraft and Model Perspective; *J. Geophys. Res.* **2003**, *108*, 4804.
19. Zhang, M.; Uno, I.; Sugata, S.; Wang, Z.; Byun, D.; Akimoto, H. Numerical Study of Boundary Layer Ozone Transport and Photochemical Production in East Asia in the Wintertime; *Geophys. Res. Lett.* **2002**, *29,* 11.
20. Wang, T.; Ding, A.; Gao, J.; Wu, W.S. Strong Ozone Production in Urban Plumes from Beijing, China; *Geophys. Res. Lett.* **2006**, *33*, L21806.
21. Dan, M.; Zhuang, G.; Li, X.; Tao, H.; Zhuang, Y. The Characteristics of Carbonaceous Species and Their Sources in $PM_{2.5}$ in Beijing; *Atmos. Environ.* **2004**, *38,* 3443-3452.
22. Wang, X.; Li, J. A Numerical Simulation Study of PM_{10} Pollution in Beijing during Summertime (in Chinese); *Acta Scientiarum Naturalium, Universitatis Pekinensis* **2003**, *39,* 251-427.
23. Yu, S.; Zhang, Y.; Xie, S.; Xie, Z.; Zeng, L.; Zheng, M.; Salmon, L.G.; Shao, M; Slanina, S. Source Apportionment of $PM_{2.5}$ in Beijing by Positive Matrix Factorization; *Atmos. Environ.* **2006**, *40,* 1526-1537.
24. Kain, J.S.; Fritsch, J.M. Convective Parameterization for Mesoscale Models: the Kain-Fritsch Scheme. In *The Representation of Cumulus Convection in Numerical Models*; Emanuel, K.A., Raymond, D.J., Eds. American Metrological Society: Boston, MA, 1993.
25. Zhang, D.L.; Anthes, R.A. A High-Resolution Model of the Planetary Boundary Layer-Sensitive Tests and Comparisons with SESAME-79 Data; *J. Appl. Meteor.* **1982**, *21*, 1594-1609.
26. Reisner, J.; Rasmussen, R. J.; Bruintjes, R.T. Explicit Forecasting of Supercooled Liquid Water in Winter Storms Using the MM5 Mesoscale Model; *Quart. J. Roy. Meteor. Soc.* **1998**, *124*, 1071-1107.
27. Dudhia, J. A Non-Hydrostatic Version of the Penn State/NCAR Mesoscale Model: Validation Tests and Simulation of an Atlantic Cyclone and Cold Front; *Mon. Weather Rev.* **1993**, *121,* 1493-1513.
28. Blackadar, A.K. Modeling the Nocturnal Boundary Layer. In *Proceedings of the Third Symposium on Atmospheric Turbulence, Diffusion and Air Quality*, American Metrological Society: Boston, MA, 1976; pp 46-49.
29. Deardorff, J.W. Efficient Prediction of Ground Surface Temperature and Moisture, with Inclusion of a Layer of Vegetation; *J. Geophys. Res.* **1978**, *83,* 1889-1903.
30. Wesely, M.L. Parameterization of Surface Resistances to Gaseous Dry Deposition in Regional-Scale Numerical Models; *Atmos. Environ.* **1989**, *23,* 1293-1304.
31. Walcek, C.J.; Aleksic, N.M. A Simple but Accurate Mass Conservative Peak-Preserving, Mixing Ratio Bounded Advection Algorithm with Fortran Code; *Atmos. Environ.* **1998**, *32,* 3863-3880.

About the Authors

Joshua S. Fu is an associate professor in the Department of Civil and Environmental Engineering at the University of Tennessee–Knoxville. David G. Streets is a senior scientist at the Argonne National Laboratory. Carey J. Jang is a senior environmental scientist at the Office of Air Quality Planning and Standards of the U.S. Environmental Protection Agency. Jiming Hao is a professor, Kebin He is a professor, and Litao Wang is a postdoctoral fellow at the Tsinghua University. Qiang Zhang is a postdoctoral fellow at the Argonne National Laboratory. Please address correspondence to: Joshua S. Fu, Department of Civil and Environmental Engineering, University of Tennessee, Knoxville, TN 37996-2010; phone +1-865-974-2629; fax: +1-865-974-2669; e-mail: jsfu@utk.edu.